

## BUAA INERTIAL TERRAIN-AIDED NAVIGATION (BITAN) ALGORITHM

Z. Chen, P. J. Yu, H. Yang

Automatic Control Department

Beijing University of Aeronautics and Astronautics

Beijing, China

### Abstract

BUAA Inertial Terrain-Aided Navigation (BITAN) algorithm is presented in this paper, which is based on Sandia Inertial Terrain-Aided Navigation (SITAN) algorithm, but several improvements from theoretic and algorithmic aspects are made as follows: (1) local observability concept is firstly presented and used; (2) square root Kalman filtering technique is adopted; (3) a new adaptive terrain stochastic linearization technique is developed; (4) both acquisition and track modes are investigated, in which the system models are different. BITAN system simulation are completed by Monte Carlo method. The position accuracy after updating is 50.3m. It has been shown that the BITAN algorithm presented in this paper is successful.

### I. Introduction

Sandia Inertial Terrain-Aided Navigation (SITAN) algorithm is a typical Terrain-Aided Navigation (TAN) algorithm, which uses an extended Kalman filter (EKF) and a local linearization technique to implement a recursive algorithm.<sup>(1)</sup> BUAA (Beijing University of Aeronautics and Astronautics) Inertial Terrain-Aided Navigation (BITAN) algorithm is a new-developed one by BUAA. The principal mechanism and applicable extent for BITAN is analogous to SITAN, but several significant improvements from theoretic and algorithmic aspects are made as follows. (1) Local observability concept are firstly presented and used in BITAN to determine the terrain-aided effectiveness qualitatively and quantitatively. (2) Square root Kalman filtering technique is adopted, which is more efficacious for one dimension (1-D) measurement case, such as TAN application. (3) A new developed Terrain Stochastic Linearization (TSL) technique, namely, Two-Subgroup Fit (TSF) technique is developed in track mode to achieve excellent performance, in addition, an adaptive TSL technique to position errors is used. (4) Both acquisition and track modes are used in BITAN, in which the Kalman filter models, TSL techniques, system error models are different.

Based on BITAN algorithm the Monte Carlo method has been used in system simulations to determine the effect of BITAN algorithm.

### II Constitution and Model of BITAN System

#### System Constitution

The constitution of BITAN system is shown in Figure 1. An Inertial Navigation System (INS) aided by baro-altimeter is used to measure the navigation state vector  $\tilde{X}$ , Kalman filtering is the main tool used to fuse together the data from INS, radar altimeter, and Digital Elevation Map (DEM) to generate the optimal estimation of error state vector  $\delta\tilde{X}$  for  $X$ . Thus  $\tilde{X}$  is updated by  $\delta\tilde{X}$ , then the optimal estimation of navigation state vector  $\hat{X}$  is obtained.

In order to implement Kalman filtering 1-D measurement  $m$  is needed, which is the difference between estimated relative height  $\hat{h}_r$  and measured relative height  $\tilde{h}_r$ .  $\tilde{h}_r$  comes from the measurement of radar altimeter,  $\hat{h}_r$  is the difference between estimated height above sea level of  $\hat{h}$  from INS and terrain height of  $h_d$  from DEM based on the estimated position of  $(\hat{x}, \hat{y})$  from INS. In addition to  $m$ , terrain slopes  $h_x$  and  $h_y$  are needed for Kalman filter, which is obtained by Terrain Stochastic Linearization (TSL) technique. TSL is realized in the local fit area  $\Omega$ , which is a varying rectangular area. The centre of  $\Omega$  is  $(\hat{x}, \hat{y})$ , and the size of  $\Omega$  is adaptive to  $\sigma_x$  and  $\sigma_y$ , where  $\sigma_x$  and  $\sigma_y$  are the standard deviation of the position errors  $\delta x$  and  $\delta y$ , which comes from the Kalman filter. As shown in Figure 1, BITAN system is constituted by two main dash-line blockes, namely, sensors and computer.

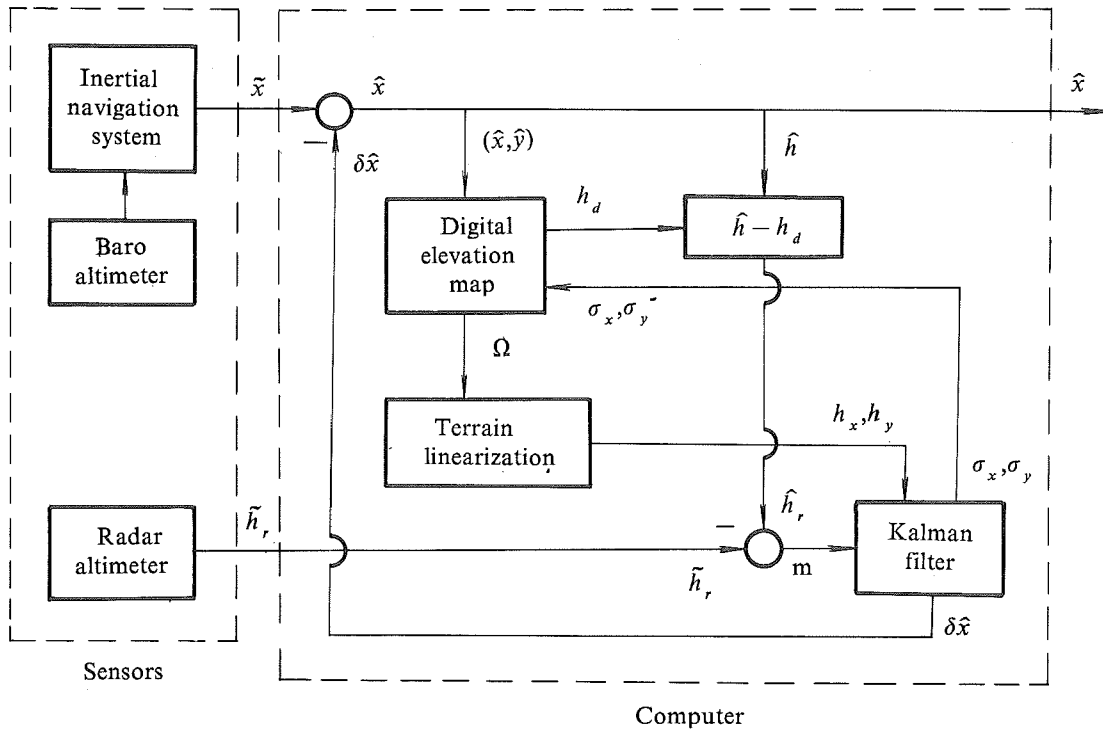


Figure 1 Block diagram of BITAN system

### System Model

The true state vector  $X$  is

$$X = [x \ y \ h \ v_x \ v_y]^T \quad (1)$$

Where  $x$ ,  $y$ , and  $h$  denote the aircraft position in a 3-D orthogonal coordinate system with three axes pointed, eastward, northward, and vertically upward, respectively, and  $v_x$  and  $v_y$  are velocities along  $x$  and  $y$  directions respectively. The error vector  $\delta X$  of  $X$  is

$$\delta X = [\delta x \ \delta y \ \delta z \ \delta v_x \ \delta v_y]^T \quad (2)$$

Therefore for a sampling period  $\tau$  the error state vector equation is as

$$\delta X(k+1) = F(\tau)\delta X(k) + W(k) \quad (3)$$

where  $F$  is the transition matrix, and  $W(k)$  the process noise vector, and

$$F(\tau) = \begin{bmatrix} 1 & 0 & 0 & \tau & 0 \\ 0 & 1 & 0 & 0 & \tau \\ 0 & 0 & 1 & 0 & 0 \\ 0 & 0 & 0 & 1 & 0 \\ 0 & 0 & 0 & 0 & 1 \end{bmatrix}, \quad W(k) = \begin{bmatrix} w_x(k) \\ w_y(k) \\ w_h(k) \\ w_{v_x}(k) \\ w_{v_y}(k) \end{bmatrix} \quad (4)$$

For a fixed  $\tau$ ,  $F(\tau)$  is a constant matrix.

With the help of Figure 1  $m$  is expressed as

$$m = \hat{h}_r - \tilde{h}_r \quad (5)$$

Let

$\hat{x}$ ,  $\hat{y}$ ,  $\hat{h}$ — estimated horizontal position and the height above sea level respectively

$h_t(\hat{x}, \hat{y})$ — true terrain height above sea level or elevation at position  $(\hat{x}, \hat{y})$

$h_d(\hat{x}, \hat{y})$ — elevation checked from DEM

Thus

$$h_d(\hat{x}, \hat{y}) = h_t(\hat{x}, \hat{y}) + \gamma_m \quad (6)$$

where  $\gamma_m$  is the mapping noise of DEM. Therefore  $\hat{h}_r$  is expressed as

$$\hat{h}_r = \hat{h} - h_d(\hat{x}, \hat{y}) \quad (7)$$

However  $\tilde{h}_r$  from radar altimeter is

$$\tilde{h}_r(x, y) = h_r(x, y) + \gamma_r \quad (8)$$

where

$(x, y)$ — true horizontal position of the aircraft

$h_r$ — true relative height

$\gamma_r$ — measurement noise of radar altimeter

Substituting above equations into Eq. (5)  $m$  is given by

$$\begin{aligned} m &= \hat{h} - h_d(\hat{x}, \hat{y}) - \tilde{h}_r(x, y) \\ &= h + \delta h - [h_t(x + \delta x, y + \delta y) + \gamma_m] \\ &\quad - (h_r + \gamma_r) \end{aligned} \quad (9)$$

Obviously,  $h_t(x,y)$  is an arbitrary curved surface function of  $(x,y)$ . To realize terrain stochastic linearization means to replace the curved surface by a plane. For example, to develop  $h_t(x+\delta x, y+\delta y)$  by one order Taylor expansion method at point  $(x,y)$ , therefore

$$h_t(x+\delta x, y+\delta y) = h_t(x,y) - \frac{\partial h_t(x,y)}{\partial x} \delta x - \frac{\partial h_t(x,y)}{\partial y} \delta y + \gamma_L \quad (10)$$

where  $\gamma_L$  is the linearization noise and

$$h_x = \frac{\partial h_t(x,y)}{\partial x}, \quad h_y = \frac{\partial h_t(x,y)}{\partial y} \quad (11)$$

are the terrain slopes along the directions of  $x$  and  $y$  respectively. Substituting Eq. (10) and (11) into Eqs.(9), and considering  $h - h_r - h_t(x,y) = 0$ , then

$$\begin{aligned} m &= h - h_r - h_t(x,y) - h_x \delta x - h_y \delta y \\ &\quad + \delta h - \gamma_m - \gamma_r - \gamma_l \\ &= -h_x \delta x - h_y \delta y + \delta h + \gamma \end{aligned} \quad (12)$$

where

$$\gamma = -\gamma_m - \gamma_r - \gamma_l \quad (13)$$

$$M = \begin{bmatrix} -h_x(k) & -h_y(k) & 1 & 0 & 0 \\ -h_x(k+1) & -h_y(k+1) & 1 & -h_x(k+1)\tau & -h_y(k+1)\tau \\ -h_x(k+2) & -h_y(k+2) & 1 & -2h_x(k+2)\tau & -2h_y(k+2)\tau \\ -h_x(k+3) & -h_y(k+3) & 1 & -3h_x(k+3)\tau & -3h_y(k+3)\tau \\ -h_x(k+4) & -h_y(k+4) & 1 & -4h_x(k+4)\tau & -4h_y(k+4)\tau \end{bmatrix} \quad (19)$$

is the measurement noise, which consists of mapping noise  $-\gamma_m$ , radar measurement noise  $-\gamma_r$ , and linearization noise  $-\gamma_l$ . Thus the measurement is given by

$$m = [-h_x \quad -h_y \quad 1 \quad 0 \quad 0] \delta X + \gamma \quad (14)$$

Then the discrete measurement equation is defined as

$$m(k) = H(k)\delta X(k) + \gamma(k) \quad (15)$$

where the measurement matrix is

$$H(k) = [-h_x(k) \quad -h_y(k) \quad 1 \quad 0 \quad 0] \quad (16)$$

The implementation of Kalman filtering is based on Eqs. (3), (4) and (15) (16).

### III. Effectiveness Analysis of TAN

So far, it is known that the effectiveness of TAN depends on the roughness of the terrain over which the aircraft has just flown. However none of the research

workers gives a qualitative and quantitative description about the effectiveness of TAN. Local observability concept are firstly presented and used in BITAN algorithm to solve this issue.<sup>(2)</sup> It is explained as follows.

Based on Eqs. (3) and (15), if five measurement values, i. e.  $m(k), m(k+1), \dots, m(k+4)$  are involved, then

$$\begin{bmatrix} m(k) \\ m(k+1) \\ m(k+2) \\ m(k+3) \\ m(k+4) \end{bmatrix} = \begin{bmatrix} H(k) \\ H(k+1)F \\ H(k+2)F^2 \\ H(k+3)F^3 \\ H(k+4)F^4 \end{bmatrix} x(k) \quad (17)$$

Define

$$M = \begin{bmatrix} H(k) \\ H(k+1)F \\ H(k+2)F^2 \\ H(k+3)F^3 \\ H(k+4)F^4 \end{bmatrix} \quad (18)$$

as local observability matrix, which is a square matrix. Substituting Eqs.<sup>(4)</sup> and (16) into Eq.(18), therefore

It is obvious that the system is locally observable in the time period  $k$  to  $k+4$ , if only if the matrix  $M$  is nonsingular. Eq. (19) shows that the observability of TAN system is highly dependent on terrain slopes  $h_x$  and  $h_y$ . By examining the elements of  $M$ , the qualitative analysis of the effectiveness of TAN is revealed as follows.

(1) To have good local observability, terrain slopes  $h_x$  and  $h_y$  cannot be too small. That is, local terrain cannot be too flat, such as plains and sea.

(2) To be observable,  $h_x(k)$  and  $h_y(k)$  must not be equal to each other. That is, the slopes along  $x$  and  $y$  directions are not the same.

(3) To be observable,  $h_x(k)$  and  $h_y(k)$  must not be equal to each other. That is, the slopes along  $x$  and  $y$  directions are not the same.

(4) From Eq. (16) one sees that when the error state  $\delta X$  is locally observable, the observability degree for all

the state variables is different. For example,  $\delta h$  has the strongest observability, since the height of the aircraft is directly measured by the radar altimeter. State variables  $\delta x$  and  $\delta y$  are observable through the terrain slope variation. State variables  $\delta v_x$  and  $\delta v_y$  have the weakest observability since they are not directly involved in the measurement matrix  $H(k)$ , but are coupled to other state variables through the system matrix  $F$ , as shown in the results of covariance analysis in Reference (2).

The quantitative description of the observability degree of TAN can be made by the condition number  $c$  of the square matrix  $M$  as

$$c = \max_j \|m_j\| \cdot \|\bar{m}_j\| \quad (20)$$

where  $m_j$  is the  $j$ -th column vector of  $M$ ,  $\bar{m}_j$  is the  $j$ -th column vector of  $M^{-1}$ , and  $\|\cdot\|$  denotes vector norm. If the condition number is large, the matrix is close to singular. The condition number of a unity matrix is 1, and that of any matrix is greater or equal to 1. Thus the larger the condition number is, the worse the observability is, and vice versa.

The condition number curves for Path 1 and Path 2 are compared in Figure 2, where Path 2 has stronger terrain roughness than Path 1. From Figure 2 following aspects are depicted.

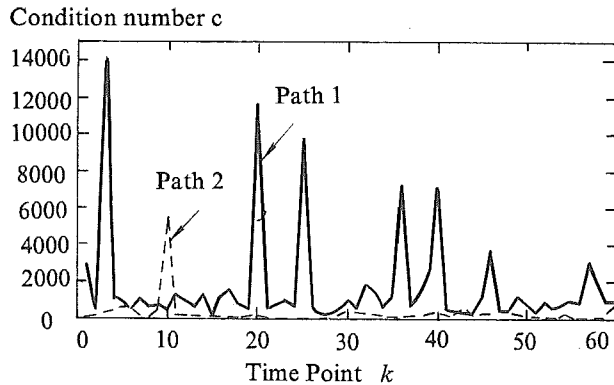


Figure 2. Two condition number curves for Path 1 and Path 2

(1) Different flight paths can be compared by means of condition number from the point of view of observability degree, namely, the updating effectiveness of TAN.

(2) Even in the same flight path from section to section, the observability degree is different, one may choose suitable flight section to implement terrain updating.

(3) Results from a good many computations indicate that the condition number of  $c=1000$  may be considered as the threshold between the strong and weak observabilities for TAN application. This threshold

may be used to choose the terrain updating area.

#### IV. Square Root Kalman Filtering

For the EKF techniques of TAN in BITAN, the dimension number of state variables is five, and that of the measurement is only one. It is very effective to adopt square root Kalman filtering technique to increase the convergence of Kalman filtering, to minimize the roundoff errors, and to improve the accuracy of terrain updating. This technique is applied in BITAN algorithm.

Let the mean value and variance of process noise  $W(k)$ , or abbreviated  $W_k$ , are

$$E[W_k] = 0 \quad (21)$$

$$E[W_k W_k^T] = U_k U_k^T \quad (22)$$

where  $U_k$  is the square root of the variance of  $W_k$ .

Let the mean value and variance of  $\gamma(k)$ , or abb.  $\gamma_k$ , are

$$E[\gamma_k] = 0 \quad (23)$$

$$E[\gamma_k^2] = R_k \quad (24)$$

where  $R_k$  is the variance of  $\gamma_k$ .

Therefore the algorithm of square root Kalman filtering is obtained as follows.

##### Time Updating

$$\delta X_{k/k-1} = F_k \delta X_{k-1} \quad (25)$$

$$\begin{bmatrix} S_{k/k-1}^T \\ 0 \end{bmatrix} = L \begin{bmatrix} S_{k-1}^T F_k^T \\ U_{k-1}^T \end{bmatrix} \quad (26)$$

where

$\delta_k$ —estimated value of error state vector

$\delta X_{k/k-1}$ —the first step predictive value of error state vector

$S_k$ —the square root of error covariance of  $\delta X_k$

$S_{k/k-1}$ —the square root of error covariance of  $\delta X_{k/k-1}$

$L$ —orthogonal matrix

##### Measurement Updating

$$X_k = X_{k/k-1} + K_k [m_k - H_k X_{k/k-1}] \quad (27)$$

$$S_k = S_{k/k-1} - r K_k B_k^T \quad (28)$$

$$K_k = \mu S_{k/k-1}^T B_k \quad (29)$$

$$B_k = S_{k/k-1}^T H_k^T \quad (30)$$

$$\frac{1}{\mu} = B_k^T B_k + R_k \quad (31)$$

$$r = \frac{1}{(1 + \sqrt{\mu \cdot R_k})} \quad (32)$$

where

$K_r$  — the optimal gain of Kalman filter

Computing Steps of  $S_{k/k-1}^T$

Eq. (26) is expressed as

$$L \cdot A = \begin{bmatrix} W \\ 0 \end{bmatrix} \begin{matrix} n \\ n \end{matrix} \quad (33)$$

$$L = L^{(n)} \cdot L^{(n-1)} \dots L^{(1)} \quad (34)$$

where  $L^{(k)}$  is an orthogonal matrix with the order of  $2n \times 2n$ ,  $n$  is the order of matrix  $F$ . Then

$$L^{(k)} = I - \beta_k u^{(k)} u^{(k)T} \quad (35)$$

$$\beta_k = \frac{2}{u^{(k)T} u^{(k)}} \quad (36)$$

Let

$$A^{(1)} = A$$

$A^{(k)}$  = the  $j$ -th column of  $A^{(k)}$

$A_{ij}^{(k)}$  — the element of the  $i$ -th row and the  $j$ -th column in  $A^{(k)}$

For  $k = 1, 2, 3, \dots, n$  following recursion formula is used:

$$A^{(k+1)} = L^{(k)} \cdot A^{(k)} \quad (37)$$

At the  $k$ -th step, the elements below the diagonal elements for the first  $(k-1)$  columns in  $A^{(k)}$  are zero, so that when  $k = n$ , there is

$$A^{(n+1)} = \begin{bmatrix} W \\ 0 \end{bmatrix} \begin{matrix} n \\ n \end{matrix} \quad (38)$$

whereas  $A^{(k+1)}$  can be determined by the following recursion formulas for  $k = 1, 2, 3, \dots, N$ :

$$\alpha_k = \sqrt{\sum_{i=k}^N (A_{ik}^{(k)})^2} \operatorname{sgn}(A_{kk}^{(k)}) \quad (39)$$

$$\beta_k = \frac{1}{\alpha_k (\alpha_k + A_{kk}^{(k)})} \quad (40)$$

$$u_i^{(k)} = \begin{cases} 0 & i < k \\ \alpha_k + A_{kk}^{(k)} & i = k \\ A_{ik}^{(k)} & i > k \end{cases} \quad (41)$$

$$V_i^{(k)} = \begin{cases} 0 & i < k \\ 1 & i = k \\ \beta_k U^{(k)T} A^{(k)} & i > k \end{cases} \quad (42)$$

$$A^{(k+1)} = A^{(k)} - U^{(k)} V^{(k)T} \quad (43)$$

Thus matrix  $S_{k/k-1}^T$  is obtained.

From Eqs. (25) to (32) and Eqs. (39) to (43) the square root Kalman filtering algorithm is implemented. Its effect may be shown in part VII of this paper.

## V. Adaptive Terrain Stochastic Linearization

As has been explained before that the effect of TSL<sub>r</sub> technique is to derive a plane function  $f(x,y)$  to replace an arbitrary curved surface function  $h_r(x,y)$  where  $h_r(x,y)$  is the terrain elevation profile above sea level at position point  $(x,y)$ . Obviously  $h_r(x,y)$  is a nonlinear function of  $x$  and  $y$ .  $f(x,y)$  is the linearized profile near the position  $(\hat{x}, \hat{y})$ , which is related to  $h(x,y)$  at the fit area  $\Omega$  via

$$f(x,y) = a + h_x(x - \hat{x}) + h_y(y - \hat{y})$$

where  $a$  is an estimated elevation at  $(\hat{x}, \hat{y})$ ,  $h_x$  and  $h_y$  are the slopes of this plane along directions  $x$  and  $y$  respectively.

In BITAN algorithm two improvements about TSL technique are involved. The one is to choose fit area  $\Omega$  adaptively to the standard deviation of the position errors, the other is to adopt a new TSL technique for TAN.

### Adaptively Choosing Fit Area $\Omega$

TSL is realized at the local fit area  $\Omega$ , whose centre is the estimated position  $(\hat{x}, \hat{y})$ . Then the local fit area  $\Omega$  is chosen as a rectangular patch of  $5\sigma_x \times 5\sigma_y$  adaptively, where  $\sigma_x$  and  $\sigma_y$  are the standard deviation of the position errors  $\delta x$  and  $\delta y$ . As shown in Figure 1  $\sigma_x$  and  $\sigma_y$  are come from the covariance analysis of Kalman filtering.  $\Omega$  is shown in Figure 3, where P is the position point for  $(\hat{x}, \hat{y})$ .

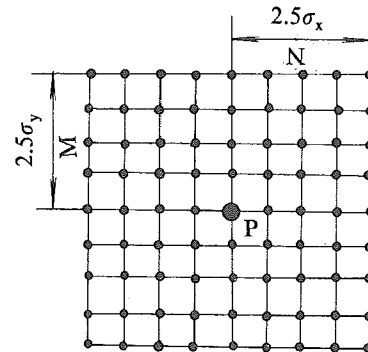


Figure 3 Ground patch geometry for local fit area  $\Omega$

The reasons to make the choice in Figure 3 is as follows.

(1) As shown in Eq.(11) that one has to determine the slopes  $h_x$  and  $h_y$  at the true position  $(x,y)$  of the aircraft, other than  $(\hat{x},\hat{y})$ . Unfortunately true position is unknown, only  $(\hat{x},\hat{y})$  is the optimum estimation for  $(x,y)$ . Thus one turns to determine the local fit area  $\Omega$ , to make  $(x,y)$  in it with very high probability. Because  $\sigma_x$  and  $\sigma_y$  are the standard deviations of  $\delta x$  and  $\delta y$ , which are the standard deviations of  $\hat{x}$  and  $\hat{y}$  too. The area  $\Omega$  for  $(\hat{x} - 2.5\sigma_x, \hat{x} + 2.5\sigma_x)$  and  $(\hat{y} - 2.5\sigma_y, \hat{y} + 2.5\sigma_y)$  is the possible area for the true aircraft position.

(2) At the begining of Kalman filtering  $\sigma_x$  and  $\sigma_y$  are much larger, but as time goes on, they become smaller.  $\Omega$  is varied with  $\sigma_x$  and  $\sigma_y$ .  $\Omega$  is chosen adaptively as shown in Figure 3.

(3) Consider  $\Omega$  is the possible area for true position, the mean weight principle in area  $\Omega$  is used for implementing TSL, other than the Gaussian weight principle as shown in Reference (3).

#### Two-Subgroup Fit (TSF) Technique

Two-Subgroup Fit (TSF) technique is firstly presented and used in BITAN algorithms, which is explained in brief as follows (for further details see Reference (4)).

At first consider fitting a straight-line into a set of data points on a plane. Dividing the points in  $\Omega$  into two subgroups, each contains half of total data points. Assuming each point carries a unity weight, locate the centre of masses for each subgroup. The line connecting the two centres of masses is the desired straight-line fit to the data set.

Extending this concept to the fitting of a plane into a set of data points two slopes for the profile are needed. Use the same geometry patch as shown in Figure 3. Divide the patch into left and right half-patches for computing slopes  $h_x$ , and into upper and lower half-patches for computing slope  $h_y$ . The set of computation equations with discrete type are

$$a = \frac{1}{(2N+1)(2M+1)} \sum_{\substack{k_x = i-N, i+N \\ k_y = j-M, j+M}} h_d(k_x, k_y) \quad (44)$$

$$h_x = \frac{1}{N(N+1)(2M+1)} \left[ \sum_{\substack{k_x = i+1, i+N \\ k_y = j-M, j+M}} h_d(k_x, k_y) - \sum_{\substack{k_x = i-N, i-1 \\ k_y = j-M, j+M}} h_d(k_x, k_y) \right] \quad (45)$$

$$h_y = \frac{1}{M(M+1)(2N+1)} \left[ \sum_{\substack{k_x = j+1, j+M \\ k_y = i-N, i+N}} h_d(k_x, k_y) - \sum_{\substack{k_x = j-M, j-1 \\ k_y = i-N, i+N}} h_d(k_x, k_y) \right] \quad (46)$$

where  $k_x$  and  $k_y$  are the sequence numbers of the grid points of DEM in fit area  $\Omega$ ,  $i$  and  $j$  are the sequence numbers of point coordinates  $\hat{x}$  and  $\hat{y}$ .

Eqs. (44) to (46) involves  $12MN+4(M+N) - 2$  additions and 8 multiplications.

Compared with other five TSL techniques given in Reference (4). TSF technique is attractive in all measure, including good accuracy, fast convergence, short computer time, and good normality, etc. Therefore this technique is recommended for both acquisition and track modes, although Nine-Point-Plane Fit (NPF) technique is sometimes used in track mode.

### VI. Acquisition and Track Modes

Both acquisition and track modes are used in BITAN algorithm. Several aspects are discussed as follows.

#### Kalman Filter Models

The Kalman filter model for track mode is shown by Eqs. (3), (4) and (15), (16). Whereas the one for acquisition mode is shown as

$$\begin{bmatrix} \delta x \\ \delta y \\ \delta y \end{bmatrix}_{k+1/j} = \begin{bmatrix} 1 & 0 & 0 \\ 0 & 1 & 0 \\ 0 & 0 & 1 \end{bmatrix}_{k/j} + W_k \quad (47)$$

$$m_k = [h_x \quad h_y \quad 1] \begin{bmatrix} \delta x \\ \delta y \\ \delta h \end{bmatrix}_{k/j} + \gamma_k \quad (48)$$

where  $j$  is the number of the parallel filter.

#### TSL Techniques

The TSL technique used in track mode is TSF technique as shown by Eqs. (44) to (46). However the one used in acquisition mode may be either the same as TSF technique or NPF technique.

NPF technique evaluates the slopes at position  $P(i,j)$  using DEM data at nine points of  $P_1$  to  $P_9$ , as shown in Figure 4, for which the patch area is  $3\sigma_x \times 3\sigma_y$ . The fit

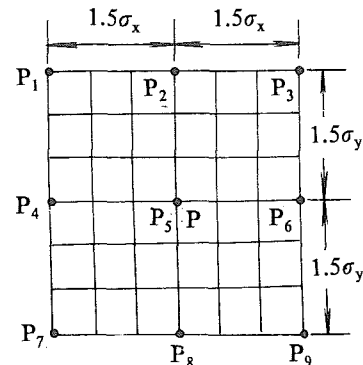


Figure 4 Ground patch geometry for NPF technique

principle is to make the quadratic sum of the fit errors at 9 points minimum. The set of computation equations with discret type are<sup>(4)</sup>

$$a = \frac{1}{9}(h_1 + h_2 + \dots + h_9) \quad (49)$$

$$h_x = \frac{1}{6d}(h_3 + h_6 + h_9 - h_1 - h_4 - h_7) \quad (50)$$

$$h_y = \frac{1}{6d}(h_7 + h_8 + h_9 - h_1 - h_2 - h_3) \quad (51)$$

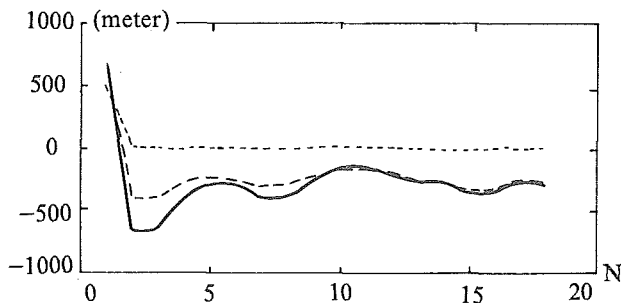
where  $h_1$  to  $h_9$  are the values of elevation  $h_d$  at points  $P_1$  to  $P_9$ . Eqs (49) to (51) involves 18 additions and 4 multiplications. Compared with the computing amount involved in TSF technique, NPF technique has much less computing amount, almost one third of computing time as TSF technique. That is why the NPF technique is sometimes used in acquisition mode.

#### System Error Models

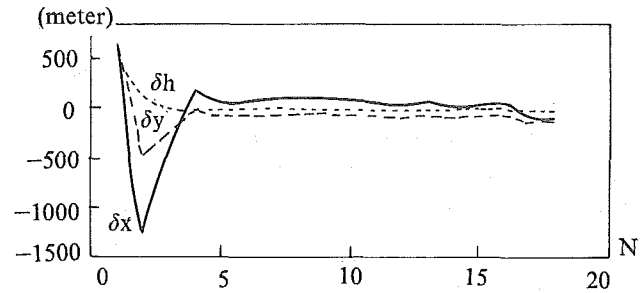
The system error models for acquisition and track modes are different. For acquisition mode 3-D process noises for  $\delta x$ ,  $\delta y$  and 1-D measurement noise  $\gamma$  are taken into account, and all of them are considered as white noises. However, for track mode two cases are considered in BITAN algorithm.

(1) If the accuracy requirement is not very high for TAN, 5-D process noises for  $\delta x$ ,  $\delta y$ ,  $\delta h$ ,  $\delta v_x$ ,  $\delta v_y$  and 1-D measurement noise  $\gamma$  are taken into account and all of them are considered as white noises.

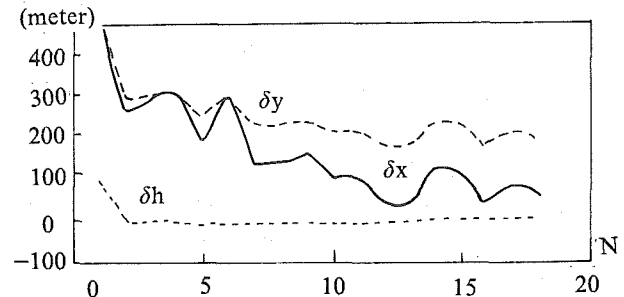
(2) If the accuracy requirement is considerable high, some process noise or measurement noise are considered as one-order Markov process noises. They are determined by the results of all-state simulation of BITAN system. For a given TAN applications two kinds of systems are modelled and simulated. One is seven-order TAN system, in which the two horizontal position noises are considered as one-order Markov process noises. Another is six-order TAN system, in which measurement noise is augmented. The simulation results are shown in Figure 5, where N is filtering number.



(a) Five-order TAN system



(b) Seven-order TAN system



(c) Six-order TAN system

Figure 5 Comparisons of the updating for TAN systems

Compared with five-order system, the seven-order system may improve the system accuracy to a large extent. However, the improvement made by the six-order system is not so encouraging. Therefore it may reasonable to consider the measurement noise as white one for TAN application.<sup>(5)</sup>

## VII. Simulation Results of BITAN System

Monte Carlo method is used to the simulation of BITAN system

#### Simulation Conditions

The simulation conditions for a given TAN system are considered as follows.

(1) Sub-optimal Kalman filtering with 3-D position errors, which are decorrelated, is adopted.

(2) The weight coefficient of measurement noise is 1.

(3) TSF linearization technique is adopted for both acquisition and track modes to obtain  $h_x$  and  $h_y$ , the size of  $\Omega$  is  $5\sigma_x \times 5\sigma_y$ .

(4) 25 parallel Kalman filters are used in acquisition mode.

(5) 12 initial position errors for two flight Pathes A and B are simulated, which are shown in Table 1. The initial horizontal position error is expressed by Average Error Radius (AER), which is defined by

Table 1 The 12 initial position errors for two flight Pathes A and B

Initial error No.		1	2	3	4	5	6	7	8	9	10	11	12
Path A	$\delta x(m)$	-33.	-84.	-40.	-33.	-51.	-66.	-41.	-70.	-43.	-32.	-59.	-44.
	$\delta y(m)$	-31.	-36.	-30.	-30.	-33.	-34.	-30.	-35.	-31.	-31.	-33.	-31.
Path B	$\delta x(m)$	-5.8	0.4	0.7	3.7	-17.	-6.7	-91.	-43.	6.4	4.7	0.3	-45.
	$\delta y(m)$	-6.3	-42.	-21.	-19.	-32.	-11.	-131	-65.	-15.	-31.	-21.	-69.

$$AER = \frac{1}{m} \sum_{i=1}^m e_i \quad (52)$$

### VIII. Conclusions

where

$$e_i = \sqrt{(x_i - \hat{x}_i)^2 + (y_i - \hat{y}_i)^2} \quad (53)$$

and

$x_i, y_i$  — true position of aircraft

$\hat{x}_i, \hat{y}_i$  — error position of BITAN system

$m$  — simulation number

The two flight pathes are taken from a DEM in Liaoning Province, China. Thus 24 error cases are simulated. The AER of initial position errors before terrain updating is 934.9m.

(6) The initial velocity errors along the  $x, y$  directions are 0.5m/s and -0.4 m/s respectively.

(7) Sampling time is 2.5s.

### Simulation Results

The distribution of position error for 24 navigation end points is shown in Figure 6. From this figure it has been shown that the CEP of navigation end points is 50.3m, and the AER of them is 51.9m. Obviously, the position accuracy is improved by more than one order of magnitude. It is higher than the accuracy made by traditional TAN algorithms.

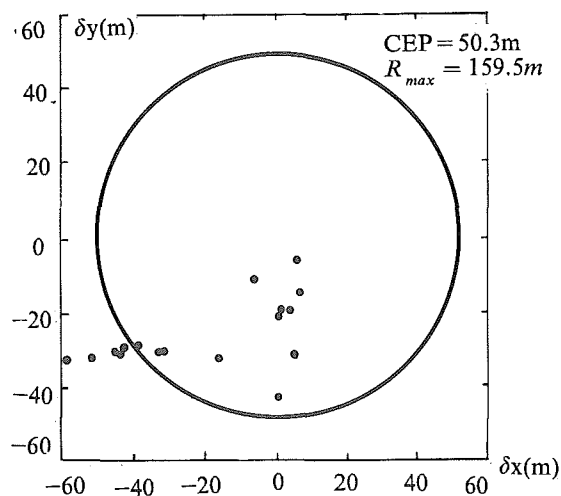


Figure 6 Position error distribution of 24 navigation end points for BITAN system

The BITAN algorithm firstly presented in this paper has made several significant improvements, such as to choose terrain updating zone by means of local observability analysis, to adopt square root Kalman filtering, to implement a new adaptive TSL technique, to use different models in different system modes, etc.. The simulation results given in this paper shows that the position accuracy given by BITAN system is 50.3m (CEP). By means of terrain updating the system accuracy is increased by more than one order of magnitude. That means BITAN algorithm is effective and successful.

### References

- (1) L. D. Hostetler and R. D. Andreas, " Nonlinear Kalman filtering techniques for terrain aided navigation, " IEEE Trans. Automat. Contr., Vol. AC 28, no.3, pp. 315-323, 1983.
- (2) Z. Chen, " Local observability and its application to multiple measurement estimation, " IEEE Trans. Industr. Electr., Vol. IE38, no.6, pp. 491-496.
- (3) R. D. Andreas, L. D. Hostetler, and R. C. Beckmann, " Continuous Kalman updating of an inertial navigation system using terrain measurement, " NAECON Rec., pp. 1263-1270, 1978.
- (4) P. J. Yu, Z. Chen, and J. C. Hung, " Performance evaluation of six terrain stochastic linearization techniques for TAN , " NAECON Rec., pp. 382-388, 1991.
- (5) Z. chen and P. J. Yu, " Model study for terrain aided navigation system, " Proceedings of IEEE International Symposium on Industrial Electronics, May 1992.